17 June 2022 To be Submitted to *Earth and Space Science*

Two Air Quality Regimes in Total Column NO_2 over the Gulf of Mexico in May 2019: Shipboard and Satellite Views

Anne M. Thompson[1,2], Debra E. Kollonige[1,3], Ryan M. Stauffer[1], Alexander E. Kotsakis[1,4], Nader Abuhassan[1,2], Lok N. Lamsal[1,2], Robert J. Swap[1], Donald R. Blake[5], Amy Townsend-Small[6], Holli D. Wecht[7]

[1]Earth Sciences Div., NASA/Goddard Space Flight Center, Greenbelt, MD 20771; anne.m.thompson@nasa.gov Orcid: 0000-0002-7829-0920; ryan.m.stauffer@nasa.gov Orcid: 0000-0002-8583-7795

[2]Univ. Maryland-Baltimore County, GESTAR and Joint Center for Earth Systems Technology, Baltimore, MD 21228;

[3]SSAI, Lanham, MD 20706 debra.e.kollonige@nasa.gov Orcid: 0000-0002-6597-328X

[4]ERT, Inc., Laurel, MD 20707; alexander.e.kotsakis@nasa.gov;

[5]Univ. California-Irvine, Dept. of Chemistry, Irvine, CA 92697, drblake@uci.edu;

[6] Univ. of Cincinnati, Dept. of Geology and Geography, Cincinnati, OH 45221-0091; townseay@ucmail.uc.edu [7] Bureau of Ocean Energy Management, Office of Environmental Programs, Sterling, VA 20166; holli.wecht@boem.gov

Three points-

- Pandora NO_2 columns and surface O_3, NO_2, CO and VOC measured on ship over the Gulf of Mexico, May 2019, displayed two air quality (AQ) regimes
- Gulf of Mexico (GOM) AQ was dominated by continental NO_2 sources and near-shore VOC; deepwater oil platforms were in a clean marine regime
- Pandora and satellite total column NO_2 over GOM agreed overall within 5% in clean, clear-sky conditions along the coast and 13% over water

Keywords: Pandora spectrometer, Pollution – Energy Sector, Gulf of Mexico, OMI NO_2

Index Terms: 0345, 0365, 1610, 1640

ABSTRACT. The Satellite Coastal and Oceanic Atmospheric Pollution Experiment (SCOAPE) cruise in the Gulf of Mexico (GOM) was conducted in May 2019 by NASA and the Bureau of Ocean Energy Management to determine the feasibility of using satellite data to measure air quality (AQ) in a region of concentrated oil and natural gas (ONG) operations. SCOAPE featured nitrogen dioxide (NO_2) instrumentation (Pandora, Teledyne API analyzer) at Cocodrie, LA (29.26°, -90.66°), and on the *Research Vessel Point Sur* operating off the Louisiana coast with measurements of ozone, carbon monoxide (CO) and volatile organic compounds (VOC). The findings: (1) both satellite and Pandora NO_2

observations revealed two AQ regimes over the GOM, the first influenced by tropical air in 10-14 May, the second influenced by flow from urban areas on 15-17 May; (2) Comparisons of OMI v4 and TROPOMI v1.3 TC (total column) NO_2 data with all Pandora NO_2 column observations on the *Point Sur* averaged 13% agreement with the largest difference during 15-17 May (~20%). At Cocodrie, LA, at the same time, the satellite-Pandora agreement was ~5%. (3) Three new-model Pandora instruments displayed a TC NO_2 precision of 0.01 Dobson Units (~5%); (4) Regions of smaller and older operations displayed high methane (CH_4) readings, presumably from leakage; VOC were also detected at high concentrations. Given an absence of regular AQ data in and near the GOM, SCOAPE data constitute a baseline against which future observations can be compared.

Plain Language Summary. The Satellite Coastal and Oceanic Atmospheric Pollution Experiment (SCOAPE) cruise in the Gulf of Mexico (GOM) conducted on the *Research Vessel Point Sur* in May 2019 investigated the feasibility of using satellite data to measure air quality in a region of concentrated oil and natural gas (ONG) operations. SCOAPE addressed both technological and scientific issues related to measuring NO_2 columns in a prototypical coastal environment. The results are as follows. First, measurements from SCOAPE demonstrated that satellite NO_2 data *can* be used to monitor ONG activity over the GOM. Second, during SCOAPE both OMI and TROPOMI TC (total column) NO_2 amounts were higher over land and sometimes the nearshore ONG-rich Gulf, than over deepwater regions farther offshore. This was confirmed by Pandora spectrometer "ground truth" TC NO_2 data measured throughout SCOAPE on shore and on ship. Third, SCOAPE established the reliability and precision of a new generation of Pandora spectrometers. Fourth, comparisons of satellite and Pandora TC NO_2 data in SCOAPE confirm previous land-water interface studies that point to limitations in satellite NO_2 in coastal regions. Finally, neither satellite nor spectrometer captures the magnitude of ambient ("nose-level") NO_2 variability in a region dotted with hundreds of ONG platforms.

1. Introduction

1.1 Background

Within the past decade, there have been several focused studies of air quality (AQ) along North American coastlines where pollutants display distinct air-water gradients due to interactions of complex marine meteorology with rapidly reacting chemical constituents. Because satellite data are viewed as fundamental to large-regional AQ observations, the sampling strategies of these campaigns include space-borne sensors that may be tested to the limit in terms of detection thresholds, accuracy and precision. Experimental designs complement the satellite observations with airborne, ship and ground-based instruments that may themselves be using technology in development. Measurements from these experiments are typically used in comparisons with satellite column amounts and, in some cases, can be used to improve the satellite retrievals. One of the

most common target species for remote sensing is nitrogen dioxide (NO_2) because it is a proxy for nitrogen oxides (NO_x = nitric oxide (NO) + NO_2), a product of combustion that is often the major precursor for the formation of ozone pollution.

Satellite, airborne and ground-based instruments for the remote sensing of NO_2 have been employed for decades. For example, satellites have been measuring NO_2 since the mid-1990s, starting with the GOME series (*Burrows et al.,* 1999). These and other long-term records, e.g. from Aura's OMI (Ozone Measuring Instrument), are well-known for characterizing global, regional and temporal variability (*Levelt et al.,* 2016; *Duncan et al.,* 2013; 2016). Seasonal patterns and trends in NO_2 as well as signatures of extreme events, e.g., the 2008-2010 recession, the 2020 COVID-19 pandemic, are well-documented (*Russell et al.,* 2012; *Tong et al.,* 2015; *Goldberg et al.,* 2020). Airborne instrumentation used to measure column amounts and profiles of NO_2 includes DOAS, e.g., GEO-TASO, GCAS (*Judd et al.*, 2020). A host of ground-based UltraViolet (UV)/Visible NO_2 instrument were intercompared in the Cabauw Intercomparison Campaign of Nitrogen Dioxide measuring Instruments (CINDI) campaigns (*Piters et al.*, 2012) and the 2019 TROpomi vaLIdation eXperiment (TROLIX; *Kreher et al.,* 2020).

1.2 Remote Sensing Studies of Coastal Air Quality/Overview of Recent Results

The Pandora spectrometer is a relatively new ground-based spectrometer (*Herman et al.,* 2009; *Herman et al.,* 2018) that has been used to measure column NO_2 in several coastal experiments: CAPABLE (*Knepp et al.* 2015) in 2010-2011; DISCOVER-AQ in Maryland in July 2011 (*Reed et al.*, 2015; *Tzortziou et al.,* 2015a); DISCOVER-AQ in Houston in 2013 (*Judd et al.,* 2019); DANCE in 2014 off the Virginia and North Carolina coast (*Martins et al.,* 2016; *Kollonige et al.,* 2018); KORUS-OC in 2016 around the Korean peninsula (*Tzortziou et al.,* 2015b; *Tzortziou et al.,* 2018; *Thompson et al.,* 2019a), OWLETS-1 in 2017 in the lower Chesapeake Bay (*Sullivan et al.,* 2018; *Gronoff et al.,* 2019), OWLETS-2 in 2018 in the upper Chesapeake Bay (*Sullivan et al.,* 2020; *Kotsakis et al.,* 2022), LISTOS (Long Island Sound) in 2018 (*Judd et al.,* 2020; *Karambelas*, 2020), LMOS in 2019 (*Stanier et al.,* 2021). **Table 1** gives a list of campaigns and experiments that preceded SCOAPE. A summary of findings from these studies follows:

- Agreement between the sun-tracking Pandora and satellite TC NO_2 with satellite varies depending on viewing geometry. The satellite footprint size at nadir is ~13x24 km for OMI and 3.5 x 7.2 km for TROPOMI. In general, agreement of Pandora TC NO_2 is closer to TROPOMI than for OMI, especially if the larger satellite pixel includes considerable spatial heterogeneity (*Thompson,* 2020; *Thompson et al.,* 2020).
- At very polluted locations, as TC NO_2 measured from the sur-

face increases, there tends to be greater disagreement with the corresponding satellite TC NO_2. (*Herman et al.,* 2019). This can be due to the heterogeneity of a region Pandora senses as polluted.

- Besides comparing NO_2 column amounts from satellite or another instrument to the Pandora, the relationship between continuous surface NO_2 and Pandora TC NO_2 in coastal environments has been investigated (*Knepp et al.,* 2015; *Martins et al.,* 2016; *Kollonige et al.,* 2018; *Thompson et al.,* 2019a). Correlations between time-coincident surface NO_2 and Pandora TC NO_2 vary considerably. Causes of the divergence may be meteorological, for example, when the Pandora senses an NO_2-rich residual layer located above a relatively unpolluted boundary layer (*Kotsakis et al.,* 2022). Cloud interferences in remotely sensed columns tend to be important along coastlines. In shipboard experiments, the in-situ instrument may be detecting plumes that are not in the field of view of the Pandora (*Thompson et al.,* 2019a).

1.3 SCOAPE Background and Scientific Issues

The Satellite Coastal and Oceanic Atmospheric Pollution Experiment (SCOAPE) cruise, designed by NASA's Goddard Space Flight Center (GSFC) and the Department of the Interior's Bureau of Ocean Energy Management (BOEM), offered an opportunity to study NO_2 pollution over the Gulf of Mexico (GOM). BOEM issues leases for oil and natural gas (ONG) exploration in the outer continental shelf (OCS) of the GOM and has jurisdiction over AQ west of 87.5°W. Based on fuel usage reported by energy, shipping and other industries over the central and western GOM, BOEM compiles estimates for NO_2, SO_2 and VOC emissions in the region (*Wilson et al.,* 2017; 2019). However, there are no AQ monitors over the GOM. In the past decade NASA has continued to refine OMI and other satellite products aimed at regional AQ (e.g., *Boersma et al.,* 2019; *Lamsal et al.*, 2014; *Lamsal et al.*, 2017; *Lamsal et al.*, 2021). At the same time, since 2018 there have been deployment of upgraded models of the Pandora instrument (*Robinson et al.,* 2020) in an effort to evaluate OMI and TROPOMI satellite products.

The SCOAPE campaign collected GOM pollution data for the first time while advancing both satellite and Pandora capabilities. A ship cruise was designed for assessing satellite capability for the measurement of trace species required to characterize GOM AQ off the eastern Louisiana coast where energy operations are heavily concentrated. In addition to BOEM's emissions data base, meteorological and logistical considerations (avoiding winter storms, late summer hurricanes) determined the sampling strategy. Onshore flow was desired to be able to detect air masses arriving from the Gulf. Because both satellite and the Pandora spectrometer operate in the near UV-Visible region, minimizing cloud cover was a criterion for logistics. May 2019 was selected; climatology shows

less cloudiness and more onshore flow in May than in June or July.

The SCOAPE cruise was planned to address the following questions:

- What do pollutant levels measured by satellite over the GOM look like, and how do deepwater regions compare to coastal Louisiana? What role does meteorology play in any observed differences? *Both satellite and shipboard measurements of total column (TC) NO_2 are used to address this question.*
- Can satellite observations detect emissions from ONG operations over the GOM and are the measurements accurate? *This is addressed by comparing TC NO_2 from satellite overpasses over the GOM with TC NO_2 from Pandora over both land and ocean.*
- How accurately do Pandora NO_2 measurements track short-term variations in emissions? How precise are Pandora TC NO_2 observations? *Pandora data are compared to shipboard NO_2 concentrations in the vicinity of ONG operations. Precision is addressed by deploying three Pandoras together 4 weeks in advance of the cruise.*
- Is there a difference in pollutant emissions between large, deepwater ONG platforms and the hundreds of small near-shore operations? *Whole-air samples collected near platforms are analyzed for VOC and other chemical tracers.*

Section 2 describes the design of the SCOAPE cruise, instrumentation and ancillary data used for analysis. **Section 3** presents results with interpretation and discussion. It turns out that the cruise period was characterized by two distinct meteorological regimes (**Section 3.1**) that were reflected in contrasting chemical composition of the GOM environment. Details of these regimes in terms of satellite and shipboard NO_2 measurements, as well as data from other pollution tracers appear in **Sections 3.2 and 3.3**. **Section 4** is a summary.

2. Experimental: Cruise Design, Operations, Instrumentation, Ancillary Data and Analysis

The cruise track for the *Research Vessel [R/V] Point Sur* is superimposed on the Google Earth Map (**Figure 1**) with land and major platform locations and color-coded NO_x emissions (*Wilson et al.*, 2019). In addition to the LOOP (Louisiana Offshore Oil Port, an exclusion zone for research operations) and heavy commercial ship traffic – fishing, energy- and non-energy-related -- there are two basic types of ONG operations in the GOM. Deep-water platforms, typically the largest and located farther from shore, are the most polluting individual operations, corresponding to locations color-coded yellow-orange-red in **Figure 1;** they primarily produce oil with accompanying natural gas flared off. Closer to shore are hundreds of older, small operations in higher-density but with less NO_x emitted per platform.

The *R/V Point Sur* departed LUMCON (Louisiana Universities Marine Consor-

tium; https://lumcon.edu) Cocodrie, LA, facility (29.26°, -90.66°) at midnight starting 10 May 2019. The ship headed east on entering the GOM, sampling in the eastern region of high-density operations (10-11 May, with the Petronius platform easternmost in **Figure 1**) before heading south and southwest toward deepwater platforms. The 10 May sampling was conducted by automated instruments only; the sea was too rough for deck work. Clouds continued through 12 and 13 May. The southernmost point of the cruise was near the Atlantis platform; legs to Brutus and back to Atlantis followed (13 May in **Figure 1**). Deepwater sampling concluded with a return to Mars/Olympus (14 May), followed by the track east and north toward Petronius (15 May revisit). The *Point Sur* headed toward the higher-density platform region to the west, sampling on 16 May. The cruise finished with a LOOP circumnavigation (17 May in **Figure 1**) before returning to LUMCON in the afternoon (local time) of 18 May 2019.

2.1. NO_2 Observations

2.1.1 OMI and TROPOMI

We use total column NO_2 observations that are available once-daily from OMI on the NASA Aura satellite (2004 to present) and from ESA's TROPOMI instrument on the Sentinel-5P satellite (2018-present). Overpasses for both satellites occur early afternoon approximately between 1300-1400 LT. OMI operates with fields of view (FOVs) varying in size from ~13 km x 24 km near nadir to ~24 km x 160 km at the outermost edges of the swath, observing direct and back scattered solar radiation between 264-504 nm needed for retrieving NO_2 column (total, tropospheric, and stratospheric) densities (*Levelt et al.,* 2006; *Boersma et al.,* 2011; *Levelt et al.,* 2018). NASA OMI NO_2 Standard Product, V3.1 (OMNO2 product; *Krotkov et al.,* 2017), validated in *Choi et al.* (2020), was available for preliminary reports on SCOAPE (*Thompson,* 2020; *Thompson et al.,* 2020). The current analysis uses the new OMI V4.0 OMNO2 data described in detail in *Lamsal et al.* (2021). Differences between V3.1 and V4.0 OMI NO_2 data include significant improvements in air mass factors (AMFs), crucial for calculating vertical column NO_2 from slant column amounts, via a new surface reflectivity product and cloud retrievals for NO_2. Specifically, the V4.0 algorithm now incorporates: (1) a new daily and OMI field of view specific geometry-dependent surface Lambertian Equivalent Reflectivity (GLER) product in both NO_2 and cloud retrievals; (2) improved cloud parameters from a new cloud algorithm (OMCDO2N) that are retrieved consistently with NO_2; and (3) a more accurate terrain pressure calculated using OMI ground pixel-averaged terrain height and monthly mean Global Modeling Initiative (GMI) terrain pressure. This product contains total, stratospheric, and tropospheric NO_2 vertical column densities (VCDs) and is available at: https://disc.gsfc.nasa.gov/datasets/OMNO2_V003/summary/. Both V3.1 and V4.0 versions of OMI NO_2 column data are presented in this work using OMI pixels with effective cloud fraction (ECF) less than 30% and quality flags indicating good data for comparisons in the GOM land-water interface.

The TROPOMI NO_2 algorithm (*van Geffen et al.* [2022] and references therein)

uses a three-step approach, initially used for the Dutch OMI NO_2 product (DOMINO; *Boersma et al.,* 2007), starting with the Differential Optical Absorption Spectroscopy (DOAS) method that determines the slant column density (SCD) with spectral information from the visible band (400-496 nm) as described by *van Geffen et al.* (2020). Individual TROPOMI NO_2 column ground pixels are 7.2 km in the along-track and 3.6 km in the across-track direction at nadir (~ 14 km wide at the edge of swath). The latest TROPOMI NO_2 algorithm improvements are described in *van Geffen et al.* (2022) including differences between v1.3 and the latest v2.1/2.2 data products. During the SCOAPE cruise and the period of the current analysis, only v1.3 offline data have been available at the European Space Agency (ESA) public data hub (https://s5phub.copernicus.eu/) so those measurements are used in this study. The TROPOMI v1.3 NO_2 product includes a combined quality assurance value (qa_value) enabling end users to easily filter data. The recommended qa_value > 0.75 for cloudy scenes and problematic retrievals was applied to the TROPOMI observations presented below.

2.1.2 In-situ Analyzers and the Pandora Spectrometer Instrument (PSI)

Surface NO_2 mixing ratios were measured by two Teledyne API T500U CAPS NO_2 instruments. For a month prior to the cruise as well as during the cruise, one CAPS instrument was situated at LUMCON as a reference for the three Pandora spectrometers being tested on the roof. The second CAPS instrument was installed in the portable trailer on the *R/V Point Sur* with other in-situ instruments (**Tables 2** and **3**). The trailer was situated on the main deck forward of the ship's exhaust stack to avoid contamination. Air was sampled via a VACUUBRAND ME1 Diaphragm Vacuum Pump and introduced into the instruments with a ~5 m sampling line.

The Pandora instrument is a ground-based UV-VIS spectroscopic instrument that provides high spectral and temporal resolution measurements of various trace gases (*Herman et al.,* 2009). In order to retrieve columnar trace gas amounts, spectra are analyzed using the Differential Optical Absorption Spectroscopy technique (DOAS; *Platt and Stutz,* 2008). Spectral measurements can be made using direct-sun/lunar (DOAS) and sky scan (Multi-Axis DOAS, MAX-DOAS) measurement modes to retrieve trace gases columns and profiles, respectively. Direct sun measurements were made during SCOAPE to ensure high temporal resolution and lower AMF uncertainties, allowing for more rigorous comparisons with space-based remote sensing measurements. Standard Pandora data products, total column O_3 and NO_2, were all processed using BlickP v1.7.16. Total column NO_2 measurements, which are used in this work, have an accuracy of 0.05 DU (2.7×10^{15} molec-cm^{-2}; *Luftblick,* 2021). All data were filtered using the L2 data quality flags (DQF) to include only data with high (0 or 10) or medium quality (1 or 11) (*Luftblick,* 2019a,b). Pandora TC NO_2 observations were resampled to 5-min averages for comparison to other measurements.

The three NASA Pandora instruments deployed for SCOAPE featured the latest

hardware and software upgrades available at that time (*Luftblick,* 2021). Each of these Pandoras (designated as P66, P67, & P68) were assembled at the same time with the most up-to-date instrument computer (Cincoze DC-1100), internal electronics (e.g. relay board, microcontroller), and tracker (LuftBlick TR1). Compared to the original tracker, the new Pandora tracker responds faster, has smoother movements, higher range of motion, and updated software for monitoring of the absolute position (*Luftblick,* 2019a,b). The advanced tracker also allows integration of a head sensor camera, enabling accurate sun tracking on a moving platform, a feature that was crucial to making high-quality column measurements onboard the *R/V Point Sur*. These data could be directly compared to satellite measurements.

In addition to the three Pandoras having similar hardware and software, the calibration approach was standardized for the instruments. Field calibration, which is necessary for accurate retrievals of total column NO_2, requires obtaining reference spectra from actual field measurements for each Pandora instrument. While the three Pandoras were collocated at LUMCON (Cocodrie, LA) for 4 weeks prior to P66 being deployed to the *R/V Point Sur*, reference spectra were selected for each instrument using data collected between 17:55:00 UTC and 18:05:00 UTC on 20 April 2019 when all three instruments sampled clear skies and low NO_2 amounts. This ensured consistency among instruments and led to very good agreement as shown in **Figure S1**. Time-matched data from P66, P67, and P68 show the reproducibility of the three Pandora instruments during the 4-week LUMCON test period, as illustrated by referencing Pandoras 66 and 68 to Pandora 67. Agreement in terms of slope and offset of the best-fit lines, as shown in the lower right box in **Figure S1,** is excellent. The correlation coefficient, R, is lower for Pandora 66 because, as the blue symbols show, the latter instrument is slightly noisier than the other two. **Figure S2** displays comparisons of the three Pandora instruments inclusive of the pre-cruise period along with Pandoras 67 and 68 that remained at LUMCON during the cruise period. Overpass comparisons for TROPOMI (gold diamonds) and OMI (magenta triangles) are also shown. Mean Pandora-TROPOMI TC NO_2 offsets are ~13% (**Figure S2)**, with the Pandora measuring higher column amounts than TROPOMI. There is more scatter among the three Pandoras during a cloudy period before the cruise on 4 through 8 May 2019.

2.2. Other Surface-based Observations

Routine meteorological parameters (temperature, relative humidity, winds), which were provided by the *Point Sur,* and continuous NO_2, O_3, CH_4, and CO_2 data were collected during SCOAPE (**Table 2).** We averaged all in-situ NO_2 observations to 5-minutes to match the 5-minute Pandora averages. Uncertainties for these instruments specified in *Martins et al.* (2016) and *Kollonige et al.* (2018) are 5% for NO_2 and 1.3% for O_3. Surface NO_2 and Pandora TC NO_2 spikes that were obviously caused by sampling of the *Point Sur* exhaust were removed from analyzed data.

Whole-air, evacuated stainless steel canisters for a large suite of VOC species,

CH_4, and CO measurements were filled 2–3 times each day on the *Point Sur* for post-cruise analyses. They were analyzed by the Rowland-Blake research group (*Colman et al.,* 2001) for a range of alkanes, alkenes, aromatics, halogenated carbon species, CO, CH_4, dimethylsulfide and other trace gases. Because of the real-time CO analyzer failure, we report CO data from the flasks only. Subsamples of each canister were transferred via vacuum line to 12 mL evacuated glass vials for stable isotope analysis (^{13}C and D) via isotope ratio mass spectrometry (IRMS) at the University of Cincinnati via the method of *Yarnes* (2013). The IRMS instrument is calibrated several times daily with standards bracketing the isotopic composition of samples and with standards matched to the concentration of samples to avoid linearity issues. The reproducibility of ^{13}C and D is 0.2‰ and 4‰, respectively.

Flask sampling on the *R/V Point Sur* was normally coordinated with a platform encounter. For large platforms, when a plume downwind was intercepted, as denoted by simultaneous NO_2 and CO_2 spikes, a flask was exposed to collect an air sample. The platform was circled and the process repeated to get an upwind sample. For smaller operations closer to shore (10-11 May and 16-17 May in **Figure 1**), plumes were more frequent and maneuvers for contrast sampling were not practical. However, when the *Point Sur* was near shore a number of flask collections were coordinated with flask fillings on land, 11-17 May, e.g. at Venice, Port Fourchon and other sites shown by red pins in **Figure 1**. Several flasks were filled during a circling of the LOOP on 17/18 May.

Boundary-layer information was supplied by Intermet-1-RSB radiosondes launched once or twice daily from 11-17 May. In most cases En-Sci electrochemical concentration cell ozonesondes were launched with the radiosondes; the ozonesonde sensing solution was the 0.5% KI, half-buffer variant (*Thompson et al.,* 2019b). The nominal launch time was midday, near the OMI and TROPOMI overpass time. On three days of the cruise, 14 May, 15 May and 17 May, ozonesondes were also launched earlier in the day when the boundary-layer height was near its daily minimum.

2.3 Meteorological Forecasts, Reanalysis and Trajectories

To monitor the meteorological conditions throughout the cruise, the Global Modeling and Assimilation Office (GMAO) provided near-real-time support (ht tps://gmao.gsfc.nasa.gov/field_campaigns/past_campaigns) with weather forecasts and data assimilation products from Global Earth Observing System (GEOS) – Forward Processing (GEOS-FP; https://fluid.nccs.nasa.gov/weathe r/) and composition forecasts with their GEOS – Composition Forecasts (GEOS-CF) products (https://fluid.nccs.nasa.gov/cf/). Both the FP and CF products were used in making fine adjustments to the cruise track as they indicated two different meteorological regimes while the *Point Sur* was sampling.

Post-analysis used the Modern-Era Retrospective analysis for Research and Applications Version 2 (MERRA-2) reanalysis, which is driven by the GEOS-5 atmospheric data assimilation system with $1/2° \times 2/3°$ resolution and 72 layers,

to demonstrate the large-scale changes in meteorological conditions during the SCOAPE cruise and the impact on the *R/V Point Sur* in transit (**Section 3.1**). To trace source regions for air arriving at the *R/V Point Sur*, we initialized 12-hour ensemble back trajectories using the Hybrid Single-Particle Lagrangian Integrated Trajectory model (HYSPLIT; https://www.arl.noaa.gov/hysplit/) developed by NOAA's Air Resources Laboratory (*Stein et al.*, 2015), driven by National Centers of Environmental Prediction (NCEP) Global Data Assimilation System (GDAS) meteorology every 3 hours at 0.5° resolution at 50 m and 500 m above sea level (**Section 3.2.3**).

3. Results and Discussion

3.1 Meteorological Overview of Two Regimes: Marine and Continental Air Masses

The GOM study region during the cruise period of 10-18 May 2019 was characterized by two distinct meteorological regimes. These consisted of primarily onshore (10 to 13/14 May; "marine") and offshore (14-18 May; "continental") flow that led to contrasts in the chemical composition. The change in large-scale conditions originated from a weak frontal system that drifted northwest to southeast through the GOM during the middle of the cruise. An illustration of the frontal system is presented in **Figure 2**, with MERRA-2 reanalysis mean sea-level pressure (MSLP; black contours), 1000 hPa wind vectors (arrows) and specific humidity (q; colors) shown for 12 UTC (06 LST) on 13 May (*Point Sur* position is the red dot). The entire 10-18 May SCOAPE track is overlaid in cyan.

The onshore flow "marine" period dominated the first few days of the cruise with easterly to southerly winds and high humidity. The 13 May snapshot shown in **Figure 2** displays the contrast in wind direction and speed, and humidity along the frontal boundary, which was analyzed as a cold front by NOAA's Weather Prediction Center (https://www.wpc.ncep.noaa.gov/archives/web_pages/sfc/sfc_archive_maps.php?arcdate=05/13/2019&selmap=2019051312&maptype=namussfc). Specific humidity values increased by nearly a factor of two from northwest (~10 g kg^{-1}) to southeast (~20 g kg^{-1}), with a corresponding change in the wind direction/source region across the front. On 13 May, the *Point Sur* (red dot on **Figure 2**) sat in a transition zone along the front and in between the two distinct air masses. This transition period is described further in **Section 3.2.3**. After 13 May, the frontal boundary pushed farther southeast into the GOM, and the wind direction became northeasterly/easterly, with trace gas measurements from the ship and satellite data indicating sources from more polluted, "continental" regions. Detailed analysis of the effects of the two large-scale meteorological regimes on the cruise pollution measurements follow in **Sections 3.2 and 3.3**.

3.2 Chemical Composition in Two Regimes: Unpolluted Marine and Moderately Polluted Continental

3.2.1 Satellite Views of Total Column (TC NO_2)

Satellite column data (TC NO_2 in **Figure 3**) capture the contrast of the two regimes. Cloud cover precluded extensive retrievals over much of the coast and open GOM on 13 May for both OMI and TROPOMI (**Figures 3a** and **3b**). The existing measurements displayed relatively low levels of TC NO_2 except for values of TC NO_2 > 0.20 DU over the New Orleans and Baton Rouge areas (red and orange in **Figures 3c** and **d**). Two days later, after the wind shift brought continental air offshore (**Figure 2**) and cloud cover retreated (mostly < 0.1 for 15 May, **Figure 3b**), the urban regions and the adjacent GOM registered widespread pixels with readings exceeding 0.15 DU TC NO_2 (**Figures 3e** and **f**). The satellite maps in **Figure 3** display overall OMI and TROPOMI similarities but detailed comparison of TC NO_2 also highlights some differences, the horizontal resolution of the two sensors being the most obvious. Individual orange-to-red pixels recorded by TROPOMI on 15 May (**Figure 3e**) may indicate NO_x sources over land and the adjacent GOM where small platforms are concentrated (**Figure 1**). However, TROPOMI retrievals run ~(0.03-0.05) DU greater than the corresponding TC NO_2 OMI readings, not only along the coast but also over GOM south of 28.5°N latitude. These differences are evaluated with the shipboard Pandora 66 (P66) and the two Pandoras (P67, P68) at LUMCON (**Section 3.3.3**).

Not all NO_2 pollution observed by satellites and on the *R/V Point Sur* during the transition of air masses on 13-14 May was from the nearby region. Starting on 13 May, the cruise encountered air originating from Mexican agricultural fires upwind of the ship. **Figure S3** shows elevated MODerate resolution Imaging Spectrometer (MODIS) aerosol optical depth (AOD) as dark reds in false color transported northward into the SCOAPE cruise region from areas of concentrated fire counts derived from MODIS and Suomi National Polar-Orbiting Partnership (Suomi NPP) Visible Infrared Imaging Radiometer Suite (VIIRS) observations (orange and red dots in Mexico). The Atmospheric Infrared Sounder (AIRS) captured elevated mid-tropospheric CO plumes from Mexico in the vicinity of the SCOAPE cruise on 13-14 May (**Figure S4**). Precise NO_2 source attribution is beyond the scope of this study, but we note that the GEOS-CF model forecast used during the cruise identified a CO-fire tracer originating from Mexico over the SCOAPE sampling region on 14 May (not shown).

3.2.2 Shipboard Measurements of Ozone and Other Trace Gases

The switch from clean marine air to a more continental influence is reflected in a number of constituents. **Figure 4a** shows that late on 13 May there was an abrupt transition in wind direction (gray line) measured on the ship from mostly south/southwest to north/northeast. Surface ozone (blue line) increased from 20 ppbv or less to more than 40 ppbv, with peak readings of >70 ppbv on 16–17 May. The lowest ozone values measured at the beginning of the cruise, 10-13 May 2019, are referred to as having air of "marine" origins (**Figure 2**). After that the air is designated as "continental" with the high-ozone levels on the last days occurring in the westernmost segment of the track (**Figure 1**). Surface CO from

shipboard canister samples (**Figure 4b**) also reflects the marine vs continental classification. Prior to 13 May, CO mixing ratios from 7 measurements range from 55-90 ppbv, levels associated with the equatorial Atlantic (*Thompson et al.,* 2000). After 13 May the canister samples range from 100 ppbv to 185 ppbv CO, with a mean value of ~130 ppbv for the period 14-18 May. Daily CO mixing ratios from the canister samples (**Figure 4b**) abruptly changed from "marine" values of ~80 ppbv to ~120 ppbv on 13 May, when the *Point Sur* encountered air parcels from the Mexican fires. Mixing ratios of CO remain elevated on 14 May when an aerosol plume from the fires was transported to the *Point Sur* (**Figure S3b**). AIRS CO (**Figure S4)** shows a similar movement of fire pollution from 13 to 14 May although much of the ship sampling area is obscured by clouds. **Figure 4b** displays shipboard surface NO_2. The overall marine vs continental contrast is present but there are many pollution spikes in the "marine" period of the cruise when the *Point Sur* was sampling near platforms, usually within 1.5-2 km. Elevated NO_2 measurements were also found between Brutus and Atlantis and southwest of the Mars/Olympus platforms (**Figure 1**).

The ozonesonde ozone mixing ratio curtain (**Figure 5**) captures the complex vertical structure of air sampled above the *Point Sur.* During the "clean marine" phase the sharp ozone gradient seen at 15 km on 12–14 May is typical of the tropopause in tropical air. The low-ozone layer between 10 and 14 km may originate from convective redistribution of air from the surface to cloud-outflow level (*Petropavlovskikh et al.*, 2010; *Thompson et al.*, 2010; *Thompson et al.,* 2012). The continental air, in contrast, that displays a tropopause closer to 10 km with ozone greater than 80 ppbv, is pervasive above 3 km. In addition, the mid-troposphere probably includes ozone of stratospheric origins, which is common in spring.

A snapshot of marine vs continental influences for CH_4, CO, CO_2 and dimethylsulfide (DMS) concentrations, based on the 27 *Point Sur* flask samples, appears in **Figure 6**. DMS is of marine biogenic origin, so it is greater in the first part of the cruise, up to 14 May, than in the latter part. Species with continental biogenic origin (isoprene, - and -pinene, not shown) exhibit the opposite pattern. **Figure 7** summarizes the relationship between ethane and CH_4 as well as ^{13}C and D for both regimes based on 15 flask samples offshore and 2 flask samples onshore (see **Figure 7b** for locations). Enhancement ratios in **Figure 7** are enhancements above mean CH_4 and ethane campaign values. Both CH_4 isotopes (**Figure 7a**) show small changes to more negative values during the shift from marine to more continental air. The highest enhancement ratios are observed after 14 May in the vicinity of the far eastern deep-water platforms (e.g., Petronius) and the far western shallow-water platforms (**Figure 7b**). This distribution is similar to previous limited GOM sampling, e.g., *Yacovitch et al.* (2020). Note that the two onshore samples show more negative ^{13}C and D compared to all the samples from the *Point Sur.*

An extreme example of air polluted with high VOC was captured in a canister sample collected near a shallow-water platform at 1612 Local Time (LT) Central

Daylight Time (CDT) on 16 May. **Figure 7a** shows that an elevated C_2H_6/CH_4 occurred with the most ^{13}C-depleted sample. **Figure 7b** depicts the location of that sample in the far western region of shallow water platforms. **Table 4** gives concentrations of representative carbon-containing compounds in the 16 May flask. The CH_4 increase was a factor of ~3 greater than the median of 27 flasks collected during the entire cruise. This concentration signified leaks from gas production; the CO_2 from the same flask was nearly identical to the all-cruise CO_2 flask median. However, ethane, n-propane and benzene amounts were 75, 130, and 45 times higher, respectively, than their cruise averages.

3.2.3 Trajectory Analysis

Although the examples in **Figures 4-7** illustrate considerable hour-to-hour variability in all the constituents measured, a contrast in overall AQ before and after 14 May 2019 dominates the chemical character of the GOM during SCOAPE. This is supported by air parcel trajectory analysis carried out with HYSPLIT driven by NCEP GDAS at 0.5° resolution. The trajectories were initialized at the start time of VOC canister sampling to help with source attribution. **Figure 8** displays ensemble 12-hour back trajectories initialized at the indicated LT (CDT) 50 m above sea level (upper panels) and 500 m (lower panels) with red, green, and blue air parcels denoting a change in release time of every 3 hours over the 12-hour period. The marine regime observed by the *Point Sur* coincides with onshore flow, indicated by winds from the south-southeast on 10-12 May as shown in **Figures 8a** and **8d** (12 May 2019 back trajectories at 0900 LT CDT) and **Figure 4a** in situ data. The continental regime observed after the start of 14 May indicates the wind shift from the north-northeast (**Figure 4a** in situ data). The corresponding trajectories appear in **Figures 8c** and **8f** on 14 May at 1700 LT CDT. May 13 marked a transition period between these two regimes. The change in wind direction viewed in **Figures 8b and 8e** captures the Mexican fire influence (southwest origins; cf **Figures S3** and **S4**) detected on the *Point Sur* prior to the 14 May shift to north-northeasterly winds on 14 May. **Figure S5** provides insight into changing winds during the continental regime, 15-17 May. During that period, back trajectories show air originating from along shore sources (e.g., shallow-water platforms, LOOP), as in the extreme pollution measured in the 16 May canister (**Figure 7** and **Table 4**).

3.3 Satellite, Pandora and Surface NO_2 During Two Regimes on SCOAPE

Figures 9 and **10** illustrate TC NO_2 variability during the SCOAPE cruise, with observations from P66, TROPOMI and OMI. **Figure 9,** that illustrates all the 5-min average P66 readings, presents a comparison of the 7 full days of SCOAPE (11-17 May). TROPOMI overpass TC NO_2 values (diamonds for color-coded days) are also shown. Transient spikes in P66 TC NO_2 that are more prevalent after the wind shift on 14 May (note the transition in the green circles after 1800 local time) signify an encounter with a local NO_2 source. Most of the P66 TC NO_2 observations on 11-13 May (red-orange, gold, purple circles) are

below 0.18 DU and no individual data point exceeds 0.20 DU. In contrast, from 15-17 May, except for the early morning, the P66 TC NO_2 readings are above 0.18 DU with most transient spikes displaying TC $NO_2 > 0.22$ DU. There is no consistent diurnal variation across the days although the proportion of spikes is greater early in the day on 15-17 May when the ship was near shore near a high density of platforms.

There were five TROPOMI overpass columns (diamonds in **Figure 9**) during the cruise, two on 11 and 13 May (orange-red and purple diamonds), that agreed within 0.03 DU of the coincident P66 TC NO_2 values. The triangles in **Figure 9** signify OMI readings for 11, 12 and 13 May 2019. The 11 and 13 May OMI TC NO_2 values (orange-red and purple triangles) are 0.02-0.03 DU lower than their TROPOMI counterparts; this is very good agreement considering the different resolution of the two satellite instruments. On 12 May, near the overpass time, 1450 local, both P66 and OMI (gold triangle) measured 0.16-0.18 DU; there was not a TROPOMI observation that day. The three TROPOMI readings on 15-17 May give TC NO_2 ~0.16 DU compared to P66 TC NO_2 values ~0.20 DU. The OMI TC NO_2 readings for 15 and 17 May are 0.17 DU, virtually the same as for TROPOMI. For both OMI and TROPOMI during the 15-17 May period, the satellite TC NO_2 measurements are ~20% lower than those of the Pandora.

Figure 10a compares P66 and satellite TC NO_2 with in-situ NO_2 observations during the cruise. The in-situ NO_2 values roughly follow the two-regime pattern, with surface NO_2 increasing ~50% after 14 May. However, most individual surface NO_2 spikes during plume encounters are not detected simultaneously by the Pandora. This can occur when the boundary layer is not well-mixed, i.e., high NO_2 trapped near the surface may not be observed in the Pandora column. Mismatches can also result when much of the NO_2 column is an above-mixed layer residual or is advected from upwind (*Thompson et al.,* 2019a). **Figure 10a** illustrates the complexity of surface-TC NO_2 relationships. For example, 15 May is the day with the greatest range in TC NO_2 values (cf **Figure 9**). There is a slow increase in P66 TC NO_2 during the morning hours (before the overpass symbols) with a few ship NO_2 spikes less than 5 ppbv (**Figure 10a**). The P66 TC NO_2 readings are in a range (0.17 ± 0.02) DU except for 4 green dots, three of them ~0.30 DU. In the afternoon of 15 May there are a number of in-situ NO_2 ship spikes > 20 ppbv, i.e. more than a 4-fold increase from the morning values. A shipboard canister sample from 15 May, ~1500 LT while passing the Petronius platform, indicated n-butane and i-pentane (species associated with flaring) that were the second highest of the campaign. However, the corresponding P66 afternoon values are confined to a 0.17-0.28 DU range, only a ~50% variation and at most a factor of 2 increase from the morning. On 16 May while passing shallow water platforms (**cf Figure 1**), the afternoon *Point Sur* shipboard spikes are higher than on 15 May (near northeastern platforms, **cf Figure 1**) but the corresponding P66 TC NO_2 measurements do not exceed 0.20 DU.

The NO_2 column densities and locations of P66 along the ship track are illus-

trated in **Figure 10b**. The location of the pre-15 May segments, mostly below 0.16 DU (green and blue dots), was in the deepwater platform area sampled with onshore winds (**Figures 2** and **8a,d,e)**. After 15 May, when P66 registered numerous segments with TC $NO_2 > 0.18$ DU, sampling was closer to shore in the vicinity of platforms like Petronius and a high-density of small natural gas operations in the northeastern and westernmost regions (orange to red in **Figure 10b**).

A summary of overpass comparisons from OMI and TROPOMI TC NO_2 relative to the shipboard Pandora 66 appears in **Figure 11**. Although the TROPOMI satellite instrument footprint is smaller than that of the OMI satellite, the offsets with P66 are nearly the same. During SCOAPE, a significant factor affecting Pandora-satellite agreement, summarized in Tables S1 and S2, was clouds. TROPOMI during 11-13 May, the cloudiest period of the cruise, recorded 20% higher TC NO_2 than the LUMCON P67 and P68 (tan-orange shaded diamonds in **Figure 11),** likely due to increased uncertainty in cloud correction in NO_2 retrievals**.** Otherwise, the satellite and Pandora TC NO_2 comparisons for clear-sky conditions agreed within 5%. A second factor influencing agreement was the satellite retrieval over water. As the P66 TC NO_2 measurements increased during 15-17 May (all symbols with Pandora TC $NO_2 > 0.19$ DU in **Figure 11**)**,** the offsets were as large as 25% (satellite data low), even in cloud-free conditions. In **Figure 11,** the satellite data with TC $NO_2 \leq 0.18$ DU averaged within 5% of the land and ship Pandoras.

4. Summary and Conclusions

The May 2019 SCOAPE cruise, conducted with the *R/V Point Sur* in a region rich in ONG activity off the Louisiana coast, has been described. Designed to determine the feasibility of using satellite data to measure AQ with TC NO_2 as the key pollutant, SCOAPE addressed both scientific and technological goals. A summary of SCOAPE findings, addressing questions posed in the Introduction, is as follows:

• *What do pollutant levels measured by satellite over the GOM look like, and how do they compare to coastal Louisiana? What role does meteorology play in any observed differences?* During our May 2019 sampling, on a regional basis, the OMI and TROPOMI satellites showed that TC NO_2 was greater over the continent and near-coastal areas than deepwater segments of the cruise. This picture of two AQ regimes, one from 10-13 May and the second from 14-18 May, was consistent with tracers measured on the ship (ozone, CO, VOC) and contrasting meteorology during the two periods.

• *Can satellite observations detect emissions from ONG operations, and are the measurements accurate?* The OMI and TROPOMI satellites detected elevated NO_2 from ONG operations on a regional basis but emissions from individual platforms could not be characterized. This limitation was due to a combination of satellite spatial resolution, once-daily overpasses, moderately high cloud cover and low to moderate pollution levels over the GOM. Referenced to both land-

and ship-based Pandoras, satellite TC NO_2 *on average* was accurate to ~5% and ~13%, respectively, with the satellite biased low at the higher pollution levels (differences ~20%). Under clear-sky conditions agreement between satellites and the Pandoras was 2-3% over the coastal site.

• *How accurately do Pandora NO_2 readings track short-term variations in ONG emissions? What is the precision of the new-model Pandora instruments that were deployed during SCOAPE?* Through most of a day's sampling, P66 TC NO_2 responds to mixed-layer NO_2 variability as measured with the ship's analyzer. However, timing and magnitude of the Pandora and in-situ NO_2 responses are typically offset due to the viewing characteristics of the spectrometer. The magnitude of one set of P66 TC NO_2 enhancement was ~50% when corresponding NO_2 plumes registered a 4-fold increase at the surface. In the first evaluation of Pandora TC NO_2 precision, three Pandora instruments, Nos. 66, 67, and 68, operating at Cocodrie, LA, for 4 weeks prior to the cruise, were found to agree within 5% (~0.01 DU) of one another.

- *Is there a difference in pollutant emissions between large, deepwater ONG platforms and*

the hundreds of small near-shore ONG operations? There were strong responses in surface and Pandora NO_2 to both deepwater and near-shore operations. The canister sampling confirmed that near-shore platforms leak methane and other VOC associated with natural gas extraction and the deepwater platforms do not because they flare the gas.

Our analysis of the SCOAPE data has not been exhaustive, leaving room for future work. For example, the LUMCON Pandora data have not been compared to surface NO_2 data or the VOC samples. Evaluating the degree to which Pandora TC NO_2 amounts correlate with surface NO_2 in the GOM is a topic for further investigation. Matching the variability to sources will require analysis with in-situ tracers, ancillary satellite data, air parcel trajectories and, where possible, model output. Better statistics for the column-surface NO_2 connection and characterization of the environmental conditions for which the link is strongest will prepare us for optimal usage of NO_2 and ozone data from the upcoming geostationary Tropospheric Emissions: Monitoring of Pollution (TEMPO) satellite instrument that is designed for hourly pollution monitoring over North American coastal waters.

Acknowledgments

We are very grateful to Capt. Nick Allen, First Mate J. D. Ellington and the entire crew of of the *R/V Point Sur* and extraordinary support and hospitality from LUMCON as well as to N Daçic (SSAI @ NASA) and V. J. Montañez-Martinez (BOEM) for on-board measurement assistance. We thank the NASA Earth Sciences Division Tropospheric Composition Program (B. Lefer) for its support of the NASA Pandora Project as well as ESA/NASA's Pandonia Global Network and Luftblick for processing the Pandora data. We acknowledge the free use of OMI tropospheric NO_2 column data from the NASA GES DISC

(doi:10.5067/Aura/OMI/DATA2017). TROPOMI data are Copernicus Sentinel data processed by ESA (doi: 10.5270/S5P-s4ljg54). This study was partially funded by the U.S. Department of the Interior, Bureau of Ocean Energy Management through Interagency Agreement M17PG00026 with NASA (B. Duncan, PI). Additional support came from the NASA HQ Applied Sciences Program (J. Haynes). All the SCOAPE data used here are available at https://www-air.larc.nasa.gov/cgi-bin/ArcView/scoape.

References

Adelman, Z. E., Pierce, R. B., Stanier, C. O., and Kenski, D. M.: LMOS: 2017 Lake Michigan Ozone Study, EM: Air and Waste Management Association's Magazine for Environmental Managers, ISSN: 2470-4741, Vol. 2020, Issue October, 2020.

Boersma, K. F., Eskes, H. J., Veefkind, J. P., Brinksma, E. J., van der A, R. J.., Sneep, M., van den Oord, G., H., J., Levelt, P. F., Stammes, P., Gleason, J. F., and Bucsela, E. J. (2007). Near-real time retrieval of tropospheric NO_2 from OMI. *Atmospheric Chemistry & Physics,* 7, 2103-2118, https://doi.org/10.5194/acp-7-2103-2007.

Boersma, K. F., Eskes, H. J., Dirksen, R. J., van der A, R. J., Veefkind, J. P., Stammes, P., et al. (2011) An improved tropospheric NO_2 column retrieval algorithm for the Ozone Monitoring Instrument, *Atmospheric Measurement Techniques*, 4, 1905–1928, https://doi.org/10.5194/amt-4-1905-2011.

Boersma, K. F., Eskes, H. J., Richter, A., De Smedt, I., Lorente, A., Beirle, S., et al. (2018) Improving algorithms and uncertainty estimates for satellite NO_2 retrievals: Results from the quality assurance for the essential climate variables (QA4ECV) project, *Atmospheric Measurement Techniques,* 11, 6651–6678, https://doi.org/10.5194/amt-11-6651-2018.

Burrows, J. P., Weber, M., Buchwitz, M., Rozanov, V., Ladstaetter-Weissenmayer, A., Richter, A., DeBeek, R., Hoogen, R., Bramstedt, K., Eichmann, K. U., Eisinger, M., Perner, D. (1999) The global ozone monitoring experiment (GOME): Mission concept and first scientific results, *Journal of Atmospheric Sciences,* 56, 151–175.

Choi, S., Lamsal, L. N., Follette-Cook, M., Joiner, J., Krotkov, N. A., Swartz, W. H., et al. (2020) Assessment of NO2 observations during DISCOVER-AQ and KORUS-AQ field campaigns, *Atmospheric Measurement Techniques*, 13, 2523–2546, https://doi.org/10.5194/amt-13-2523-2020.

Colman, J. J., A. L. Swanson, S. Meinardi, B. C. Sive, D. R. Blake and F. S. Rowland (2001). Description of the Analysis of a Wide

Range of Volatile Organic Compounds in Whole Air Samples Collected during PEM-Tropics A and B, *Analytical Chemistry*, 73 (N15), 3723-3731.

Dačic, N., Sullivan, J. T., Knowland, K. E., Wolfe, G. M., Oman, L. D., et al. (2020). Evaluation of NASA's high-resolution global composition simulations: Understanding a pollution event in the Chesapeake Bay during the summer 2017 OWLETS campaign. *Atmospheric Environment*, 222, https://doi.org/10.1016/j.atmosenv.2019.117133.

Duncan B. N. (2020) NASA resources to monitor offshore and coastal air quality. Sterling (VA): U.S. Department of the Interior, Bureau of Ocean Energy Management. OCS Study BOEM 2020-046. 41 p.

Duncan, B., Yoshida, Y., De Foy, B., Lamsal, L., Streets, D., Lu, Z., et al. (2013). The observed response of ozone monitoring instrument (OMI) NO2 columns to NOx emission controls on power plants in the United States: 2005-2011. *Atmos. Environ., 81*, 102-111, https://doi.org/10.1016/j.atmosenv.2013.08.068.

Duncan, B., Lamsal, L., Thompson, A., M., Yoshida, Y., Hurwitz, M., M., Pickering, K., E., et al. (2016). A space-based, high-resolution view of notable changes in urban NOx pollution around the world (2005-2014). *Journal of Geophysical Research, 121*(2), 976-996, https://doi.org/10.1002/2015JD024121.

Goldberg, D. L., Anenberg, S. C., Griffin, D., McLinden, C. A., Lu, Z., Streets, D. G. (2020) Disentangling the impact of the COVID-19 lockdowns on urban NO_2 from natural variability, *Geophysical Research Letters,* https://doi.org/10.1029/2020GL089269.

Gronoff, G., Robinson, J., Berkoff, T., Swap, R., Farris, B., Schroeder, J., et al. (2019), A method for quantifying near range point source induced O_3 titration events using co-located Lidar and Pandora measurements, *Atmospheric Environment,* 204, 43-52, https://doi.org/10.1016/j.atmosenv.2019.01.052.

Herman, J., Abuhassan, N., Kim, J., Kim, J., Dubey, M., Raponi, M., and Tzortziou, M. Underestimation of column NO_2 amounts from the OMI satellite compared to diurnally varying ground-based retrievals from multiple PANDORA spectrometer instruments, Atmos. Meas. Tech., 12, 5593–5612, https://doi.org/10.5194/amt-12-5593-2019.

Herman, J., Cede, A., Spinei, E., Mount, G., Tzortziou, M., and Abuhassan, N. (2009). NO2 column amounts from ground-based Pandora and MFDOAS spectrometers using the direct-sun DOAS technique: Intercomparisons and application to OMI validation*, J.*

Geophys. Res.-Atmos., 114(D13), https://doi.org/10.1029/2009JD011848.

Herman, J., Spinei, E., Fried, A., Kim, J., Kim, J., Kim, W., et al. (2018). NO_2 and HCHO measurements in Korea from 2012 to 2016 from PSI spectrometer instruments compared with OMI retrievals and with aircraft measurements during the KORUS-AQ campaign. *Atmos. Meas. Tech., 1-60*, https://doi.org/10.5194/amt-2018-56.

Judd, L. M., Al-Saadi, J. A., Janz, S. J., Kowalewski, M. G., Pierce, R. B., Szykman, J. J., et al. (2019) Evaluating the impact of spatial resolution on tropospheric NO_2 column comparisons within urban areas using high-resolution airborne data, *Atmospheric Measurement Technology,* 12, 6091–6111, https://doi.org/10.5194/amt-12-6091-2019.

Judd, L., et al. (2020), Evaluating Sentinel-5P TROPOMI tropospheric NO_2 column densities with airborne and Pandora spectrometers near New York City and Long Island Sound, *Atmospheric Measurement Techniques*, https://doi.org/10.5194/amt-2020-151.

Karambelas, A. (2020) LISTOS: Toward a better understanding of New York City's ozone pollution problem, EM Magazine (Air and Waste Management Assn), Oct 2020.

Knepp, T., et al. (2015). Estimating surface NO_2 and SO_2 mixing ratios from fast-response total column observations and potential application to geostationary missions, *Journal of Atmospheric Chemistry*, 72(3–4), 261–286, https://doi.org/10.1007/s10874-013-9257-6.

Kollonige, D. E., Thompson, A. M., Josipovic, M., Tzortziou, M., Beukes, J. P., Burger, R., et al. (2018). OMI satellite and ground-based Pandora observations and their application to surface NO_2 estimations at terrestrial and marine sites, *J. Geophys. Res. Atmos.*, 123(2), 1441-459, https://doi.org/10.1002/2017JD026518.

Kotsakis, A., Sullivan, J.T., Hanisco, T.F., Swap, R.J., Caicedo, V., Berkoff, T.A., et al. (2022) Sensitivity of total column NO_2 at a marine site within the Chesapeake Bay during OWLETS-2, *Atmospheric Environment,* 277, https://doi.org/10.1016/j.atmosenv.2022.119063.

Kreher, K., Van Roozendael, M., Hendrick, F., Apituley, A., Friess, U., Lampel, J., et al. (2017). First results of the CINDI-2 semi-blind MAX-DOAS intercomparison, *EGU General Assembly*, Vienna, Austria, 23– 28 April 2017, EGU2017-13927.

Krotkov, N. A., Lamsal, L. N., Celarier, E. A., Swartz, W. H.,Marchenko, S. V., Bucsela, E. J., Chan, K. L., Wenig,

M., Zara, M. (2017) The version 3 OMI NO_2 standard product, *Atmospheric Measurement Technology*, 10, 3133–3149, https://doi.org/10.5194/amt-10-3133-2017.

Lamsal, L. N., Krotkov, N. A., Celarier, E. A., Swartz, W. H., Pickering, K. E., Bucsela, E. J., et al. (2014). Evaluation of OMI operational standard NO_2 column retrievals using in situ and surface-based NO_2 observations. *Atmospheric Chemistry and Physics*, 14(21), 11,587–11,609, https://doi.org/10.5194/acp-14-11587-2014.

Lamsal, L. N., Janz, S., Krotkov, N., Pickering, K. E., Spurr, R. J. D., Kowalewski, M., et al. (2017) High-resolution NO_2 observations from the Airborne Compact Atmospheric Mapper: Retrieval and validation*, Journal of Geophysical Research,* 122, 1953–1970, https://doi.org/10.1002/2016JD025483.

Lamsal, L. N., Krotkov, N. A., Vasilkov, A., Marchenko, S., Qin, W., Yang, E.-S., et al. (2021) Ozone Monitoring Instrument (OMI) Aura nitrogen dioxide standard product version 4.0 with improved surface and cloud treatments, *Atmospheric Measurement Techniques,* 14, 455–479, https://doi.org/10.5194/amt-14-455-2021.

Levelt, P., Van den Oord, G., Dobber, M., Malkki, A., Visser, H., De Vries, J., et al. (2006). The ozone monitoring instrument, *IEEE Transactions on Geosci, and Remote Sensing, 44*(5), 1093-1101.

Levelt, P. F., Joiner, J., Tamminen, J., Veefkind, J. P., Bhartia, P. K., Zweers, D. C. S. et al. (2018) The ozone monitoring instrument: Overview of 14 years in space, *Atmospheric Chemistry and Physics*, 18(8):5699–5745, https://doi.org/10.5194/acp-18-5699-2018.

Luftblick (2019a) Fiducial Reference Measurements for Air Quality, available at: https://www.pandonia-global-network.org/wp-content/uploads/2021/01/LuftBlick_FRM4AQ_InstrumentChangeUpgrade_RP_2019002_v4.pdf (last access: 15 March 2021).

Luftblick (2019b) Fiducial Reference Measurements for Air Quality TN on Data Quality Flagging Generic

Procedure Evolution, available at: https://www.pandonia-global-network.org/wp-content/uploads/2022/02/LuftBlick_FRM4AQ_DataQualityFlaggingGenericProcedureEvolution_TN_2019008_v5.pdf (last access: 15 March 2021).

Luftblick (2021) Pandonia Global Network Data Products Readme Document Version 1.8-3, available at: https://www.pandonia-global-network.org/wp-content/uploads/2021/01/PGN_DataProducts_Readme_v1-8-3.pdf (last access: 15 March 2021)

Martins, D. K., Stauffer, R. M., Thompson, A. M., Knepp, T. N., Pippin, M. (2012), Surface ozone at a coastalsuburban site in 2009 and 2010: Relationships to chemical and meteorological processes,

Journal of Geophysical Research, 117, D05306, https://doi.org/10.1029/2011JD016828.

Martins, D. K., Najjar, R. G., Tzortziou, M., Abuhassan, N., Thompson, A.M., and D. E. Kollonige (2016), Spatial and temporal variability of ground and satellite column measurements of NO_2 and O_3 over the Atlantic ocean during the Deposition of Atmospheric Nitrogen to Coastal Ecosystems Experiment (DANCE), *Journal of Geophysical Research*, 121(23), https://doi.org/10.1002/2016JD024998.

Nowlan, C. R., Liu, X., Leitch, J. W., Chance, K., Gonzalez, A. G., Liu, C., et al. (2016) Nitrogen dioxide observations from the Geostationary Trace gas and Aerosol Sensor Optimization (GeoTASO) airborne instrument: Retrieval algorithm and measurements during DISCOVER-AQ Texas 2013, *Atmospheric Measurement Techniques,* 9, 2647–2668, https://doi.org/10.5194/amt-9-2647-2016.

Petropavlovskikh, I., Ray, E., Davis, S. M., Rosenlof, K., Manney, G., Shetter, R,. Hall, B., et al. (2010) Low ozone bubbles observed in the tropical tropopause layer during the TC4 campaign in 2007, *Journal of Geophysical Research*,115, D00J16, https://doi.org/10.1029/2009JD012804.

Piters, A. J. M., Boersma, K. F., Kroon, M., Hains, J. C.,Van Roozendael, M., Wittrock, F., et al. (2012) The Cabauw Intercomparison campaign for Nitrogen Dioxide measuring Instruments (CINDI): Design, execution, and early results, *Atmospheric Measurement Technology,* 457–485, https://doi.org/10.5194/amt-5-457-2012.

Platt, U. and Stutz, J. (2008) Differential Optical Absorption Spectroscopy Principles and Applications. Springer-Verlag. http://www.springer.com/environment/environmental+engineering+and+physics/book/978-3-540-21193-8

Reed, A. J., Thompson, A. M., Kollonige, D. E., Martins, D. K., Tzortziou, M. A., Herman, J. R., Berkoff, T. A., Abuhassan, N. K., and A. Cede (2015), Effects of local meteorology and aerosols on ozone and nitrogen dioxide retrievals from OMI and Pandora spectrometers in Maryland, USA during DISCOVER-AQ 2011, *J Atmos. Chem.*, 72(3-4), 455-482, https://doi.org/10.1007/s10874-013-9254-9.

Robinson, J., Kotsakis, A., Santos, F., Swap, R. J., Knowland, K. E., Labow, G., et al. (2020) Using networked Pandora observations to capture spatiotemporal changes in total column ozone associated with stratosphere-to-troposphere transport, *Atmospheric Research,* https://doi.org/10.1016/j.atmosres.2020.104872.

Russell, A.R., Valin, L. C., and R. C. Cohen (2012). Trends in OMI NO_2 observations over the United States: effects of

emission control technology and the economic recession, *Atmos. Chem. Phys.*, 12, 12197–12209, https://doi.org/10.5194/acp-12-12197-2012.

Stanier, C.O., Pierce, R.B., Abdi-Oskouei, M., Adelman, Z.E., Al-Saadi, J., Alwe, H.D., et al. (2021) Overview of The lake Michigan ozone study 2017, *Bulletin of the American Meteorological Society*, https://doi.org/10.1175/BAMS-D-20-0061.1.

Stein, A. F., Draxler, R. R., Rolph, G. D., Stunder, B. J. B., Cohen, M. D., and F. Ngan (2015). NOAA's hysplit

atmospheric transport and dispersion modeling system. *Bulletin of the American Meteorological Society, 96*(12), 2059-2077, https://doi.org/10.1175/BAMS-D-14-00110.1.

Sullivan, J. T., Dreessen, J., Berkoff, T., Delgado, R., Ren, X., Aburn, G., Jr. (2020) OWLETS -2: An Enhanced Monitoring Strategy Directly within the Chesapeake Bay, *EM Magazine* (Air and Waste Management Assn), Oct 2020.

Sullivan, J. T., Berkoff, T., Gronoff, G., Knepp, T., Pippin, M., Allen, D., et al. (2018) The Ozone Water-Land Environmental Transition Study (OWLETS): An innovative strategy for understanding Chesapeake Bay pollution events, *Bulletin of the American Meteorological Society*, https://doi.org/10.1175/BAMS-D-18-0025.

Thompson, A. M. (2020) Evaluation of NASA's remote-sensing capabilities in coastal environments. 49 p. OCS Study BOEM 2020-047. https://espis.boem.gov/final%20reports/BOEM_2020-047.pdf.

Thompson, A. M., Doddridge, B. G., Witte, J. C., Hudson, R. D., Luke, W. T., Johnson, J. E., et al. (2000) A tropical Atlantic paradox: Shipboard and satellite views of a tropospheric ozone maximum and wave-one in January-February 1999, *Geophysical Research Letters*, **27,** 3317-3320, https://doi.org/10.1029/1999GL011273.

Thompson, A. M., MacFarlane, A.M., Morris, G. A., Yorks, J. E., Miller, S. K., Taubman, B. F., et al. (2010) Convective and wave signatures in ozone profiles over the equatorial Americas: Views from TC4 (2007) and SHADOZ, *Journal of Geophysical Research: Atmospheres,* 115, D00J23, https://doi.org/10.1029/2009JD012909.

Thompson, A. M., Miller, S. K., Tilmes, S., Kollonige, D. W., Witte, J. C., Oltmans, S. J., et al. (2012) Southern Hemisphere Additional Ozonesondes (SHADOZ) ozone climatology (2005-2009): Tropospheric and tropical tropopause layer (TTL) profiles with comparisons to OMI-based ozone products. *ournal Geophysical Research*, **117,** D23301, https://doi.org/10.1029/2010JD016911.

Thompson, A.M., Stauffer, R.M., Boyle, T.P.; Kollonige, D.E., Miyazaki, K., Tzortziou, M. A., et al. (2019a) Comparison of near-surface NO_2 pollution

with Pandora total column NO_2 during the Korea-United States Ocean Color (KORUS OC) campaign, 2019, *Journal of Geophysical Research*, 124, https://doi.org/10.1029/2019JD030765.

Thompson, A. M., Smit, H. G. J., Witte, J. C., Stauffer, R. M., Johnson, B. J., Morris, G. A., et al. (2019b) Ozonesonde Quality Assurance: The JOSIE-SHADOZ (2017) Experience, *Bulletin of the American Meteorological Society,* https://doi.org/10.1175/BAMS-17-0311.

Thompson, A. M., Kollonige, D. E., Stauffer, R.M., Abuhassan, N., Kotsakis, A. E., Swap, R. J., and Wecht, H. E. (2020) Satellite and shipboard views of air quality along the Louisiana coast: The 2019 SCOAPE (Satellite Coastal and Oceanic Atmospheric Pollution Experiment) cruise, *EM Magazine* (Air and Waste Management Assn), Oct 2020.

Tong, D. Q., Lamsal, L., Pan, L., Ding, C., Kim, H., Lee, P., et al. (2015) Long-term NOx trends over large cities in the United States during the great recession: Comparison of satellite retrievals, ground observations, and emission inventories, Atmos. Environ., 107, 70–84, https://doi.org/10.1016/j.atmosenv.2015.01.035.

Tzortziou, M., Herman, J. R., Loughner, C. P., Cede, A., Abuhassan, N., and Naik, S. (2015a). Spatial and temporal variability of ozone and nitrogen dioxide over a major urban estuarine ecosystem, *J. Atmos. Chem.*, https://doi.org/10.1007/s10874-013-9255-8.

Tzortziou, M., Thompson, A. M., and J. Herman (2015b), Dynamics of atmospheric trace gases and aerosols in Korean coastal waters: Impacts on ocean color atmospheric correction and surface air pollution studies (NASA Project Description, Grant # NNX16AD60G, PI: Tzortziou).

Tzortziou, M., Parker, O., Lamb, B., Herman, J., Lamsal, L., Stauffer, R., and Abuhassan, N. (2018). Atmospheric trace gas (NO_2 and O_3) variability in Korean coastal waters, implications for remote sensing of coastal ocean color dynamics, *Remote Sens.*, 10*,* https://doi.org/10.3390/rs10101587.

van Geffen, J. H. G. M., Eskes, H. J., Boersma, K. F., Maasakkers, J. D., Veefkind, J. P. (2018). TROPOMI ATBD of the total and tropospheric NO2 data products (issue 1.2.0). Royal Netherlands Meteorological Institute (KNMI), De Bilt, the Netherlands, http://www.tropomi.eu/sites/default/files/files/publicS5P-KNMI-L2-0005-RP-ATBD_NO2_data_products-20190206_v140.pdf.

van Geffen, J., Eskes, H., Compernolle, S., Pinardi, G., Verhoelst, T., et al. (2022) Sentinel-5P TROPOMI NO_2 retrieval: impact of version v2.2 improvements and comparisons with OMI and ground-based data, *Atmospheric Measurement Techniques,* 15, 2037–2060, https://doi.org/10.5194/amt-15-2037-2022.

Veefkind, J., Aben, I., McMullan, K., Forster, H., de Vries, J., Otter, G., et al. (2012). TROPOMI on the ESA Sentinel-5 Precursor: A GMES mission for global observations of the atmospheric composition for climate, air quality

and ozone layer applications. *Remote Sens. of Environ.*, 120, 70–83, https://doi.org/10.1016/j.rse.2011.09.027.

Wilson, D. R., Billings, R., Chang, S., Enoch, B., Do, H., Perez, H., Sellers, J. (2017) Year 2014 Gulfwide emissions inventory study. US Dept. of the Interior, Bureau of Ocean Energy Management, Gulf of Mexico OCS Region, New Orleans, LA. OCS Study BOEM 2017-044. 275 pp. https://www.boem.gov/environment/environmental-studies/2014-gulfwide-emission-inventory.

Wilson, D., Billings R., Chang, R., Do, B., Enoch, S., Perez, H., and Sellers, J. (2019) Year 2017 emissions inventory study. New Orleans (LA): US Department of the Interior, Bureau of Ocean Energy Management. OCS Study BOEM 2019-072. 231 p., https://espis.boem.gov/final%20reports/BOEM_2019-072.pdf.

Yacovitch, T., Daube, C., Herndon, S. (2020) Methane emissions from offshore oil and gas platforms in the Gulf of Mexico, *Environ. Sci. Technol.* 2020, 54, 6, 3530–3538, https://doi.org/10.1021/acs.est.9b07148.

Yarnes, C. (2013), 13C and 2H measurement of methane from ecological and geological sources by gas chromatography/combustion/ pyrolysis isotope-ratio mass spectrometry, Rapid Commun. Mass Spectrom., 27, 1036–1044, https://doi.org/10.1002/rcm.6549.

Figure captions.

Figure 1. SCOAPE cruise track (black), with arrows indicating movements of *R/V Point Sur* in May 2019. Pandora calibrations were conducted at Cocodrie. Canister samples were coordinated with ship canister filling from locations in Louisiana shown as red pins.

Figure 2. MERRA-2 meteorological reanalysis output for 12 UTC (06 LST) on 13 May 2019. The *R/V Point Sur* cruise track is shown in cyan, with the location of the ship indicated by the red dot. MERRA-2 MSLP (black contours), 1000 hPa wind vectors (black arrows), and 1000 hPa specific humidity (colors) summarize the large-scale meteorological conditions encountered during the middle of the cruise.

Figure 3. OMI v4 effective cloud fraction over SCOAPE cruise region on (a) 13 May 2019 and (b) 15 May 2019. Total Column (TC) NO_2 (DU) over SCOAPE cruise region on 13 May 2019 for (c) OMI v4 and (d) TROPOMI v1.3 observations. Total Column (TC) NO_2 (DU) on 15 May 2019 for (e) OMI v4 and (f) TROPOMI v1.3. In (c) through (f) black open squares are the locations of the top 500 NO_x-emitting platforms from BOEM's 2014 inventory (*Wilson et al.,* 2017); white open squares mark the same in (a) and (b). The gray solid line marks the *R/V Point Sur* cruise track. The cities of New Orleans, Louisiana (NOLA), and Baton Rouge, Louisiana, are indicated with open gray stars.

Figure 4. (a) Ozone mixing ratio (right scale) in ppbv with wind direction (left scale, in degrees) measured on *R/V Point Sur* during May 2019 cruise (presented as 5-minute means); (b) NO_2 mixing ratio (left scale; 15-minute means) in ppbv

with CO mixing ratio in ppbv from canister samples taken along the *R/V Point Sur* track.

Figure 5. Ozonesonde profiles, during SCOAPE, based on 0.25 km resolution data. Mixing ratios to 16 km are illustrated; layers with > 80 ppbv may signify stratospheric influence. Blue colors are concentrations associated with tropical marine boundary layer. On 12-14 May ozone concentrations 20-30 ppbv above 10 km are typical of air parcels in which deep convection introduced boundary layer air.

Figure 6. Box and whisker panels for CH_4, CO, CO_2 and dimethylsulfide (DMS) before (left side of each panel) and after 14 May (right side of each panel). Sample numbers indicated at the top or bottom of each panel. Red line denotes median values, blue box denotes 25^{th} and 75^{th} percentile, and whiskers (dashed bars) are 95^{th} percentile.

Figure 7. VOC canister observations of CH_4 isotope source signatures for ship (circles) and coastal (squares) measurements 11-19 May 2019. Colormap indicates ethane to methane ratios (% (ppb/ppb)) in the scatter plot (a) and in the map (b). Error bars show 1-sigma.

Figure 8. HYSPLIT 12-hour ensemble back trajectories released at 50m (top panels; a-c) and 500m (lower panels; d-f) at the local times listed in each (12-14 May 2019) and driven by the NCEP Global Data Assimilation System (GDAS) at 0.5° resolution. Colors of the trajectories denote change in ensemble trajectories' release time (every 3 hours over 12-hour period).

Figure 9. Pandora diurnal cycle of TC NO_2 during the cruise period 11-17 May 2019 (color of lines denotes day of observation) with TROPOMI overpass values (diamonds in corresponding day of cruise color) and OMI v4 overpass values (triangles in corresponding day of cruise color).

Fig 10. (a) Time series of TROPOMI, OMI v4, Pandora TC NO_2 and in situ NO_2 during SCOAPE cruise. Pandora TC NO_2 measurements and in situ data are 5-min averages. (b) Pandora TC NO_2 along ship track (in gray), 10-18 May 2019, during SCOAPE cruise. Blue squares mark the locations of platforms that fall into the category of the top 200 NO_x emitters according to the 2014 BOEM inventory (*Wilson et al.,* 2017). The cleaner air portion of the cruise, as shown in Figures 4 and 5, was sampled prior to 14 May, more polluted air masses after 14 May.

Figure 11. Satellites vs. Pandora 66 TC NO_2 on the *R/V Point Sur* during the cruise period 11-17 May 2019 with OMI v3 (light blue circles), OMI v4 (blue triangles), and TROPOMI v1.3 (cyan diamonds) readings referred to y-axis versus Pandora 66 on x-axis. Satellites vs. Pandora TC NO_2 at LUMCON 11-17 May 2019 with: OMI v3 versus Pandora 67 (light yellow circles) and 68 (yellow circles) on the x-axis; OMI v4 versus Pandora 67 (dark green triangles) and 68 (green triangles) on the x-axis; and TROPOMI v1.3 versus Pandora 67 (gold diamonds) and 68 (tan diamonds) on the x-axis.

Figures.

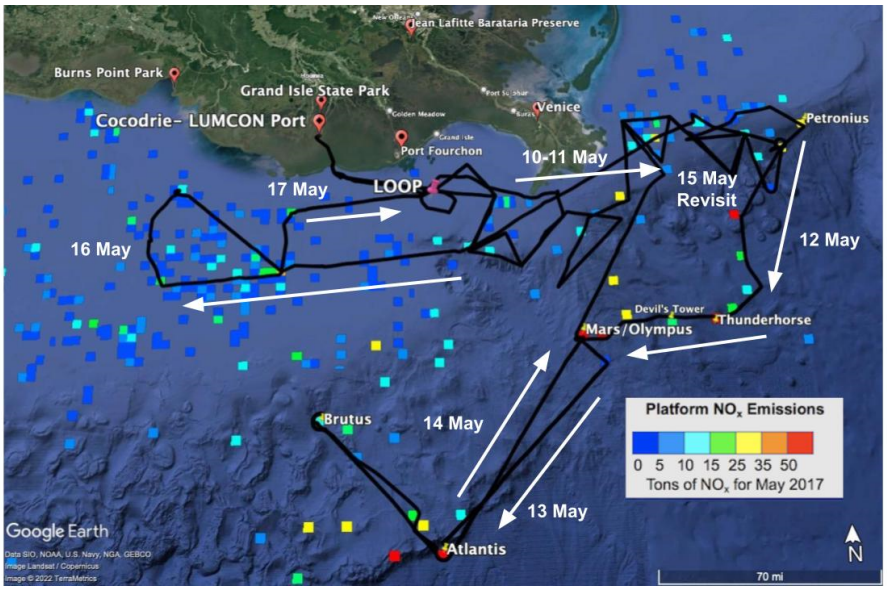

Figure 1. SCOAPE cruise track (black), with arrows indicating movements of *R/V Point Sur* in May 2019. Pandora calibrations were conducted at Cocodrie. Canister samples were coordinated with ship canister filling from locations in Louisiana shown as red pins.

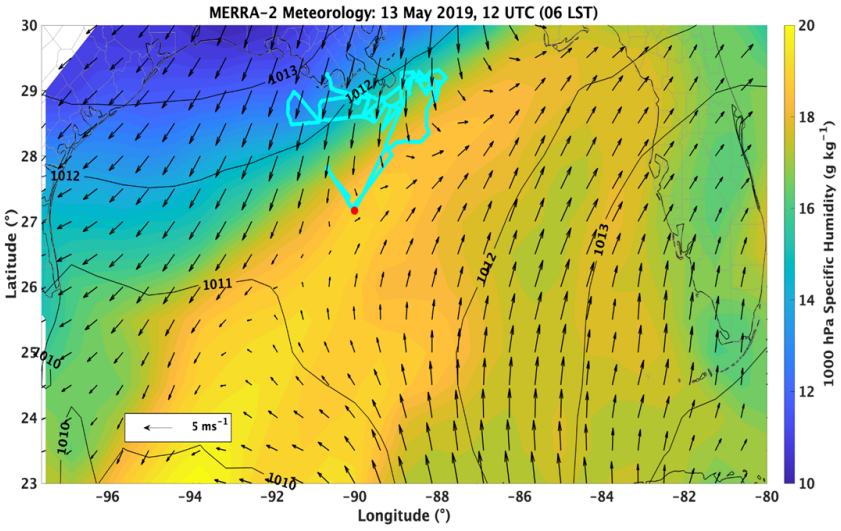

Figure 2. MERRA-2 meteorological reanalysis output for 12 UTC (06 LST) on 13 May 2019. The *R/V Point Sur* cruise track is shown in cyan, with

the location of the ship indicated by the red dot. MERRA-2 MSLP (black contours), 1000 hPa wind vectors (black arrows), and 1000 hPa specific humidity (colors) summarize the large-scale meteorological conditions encountered during the middle of the cruise.

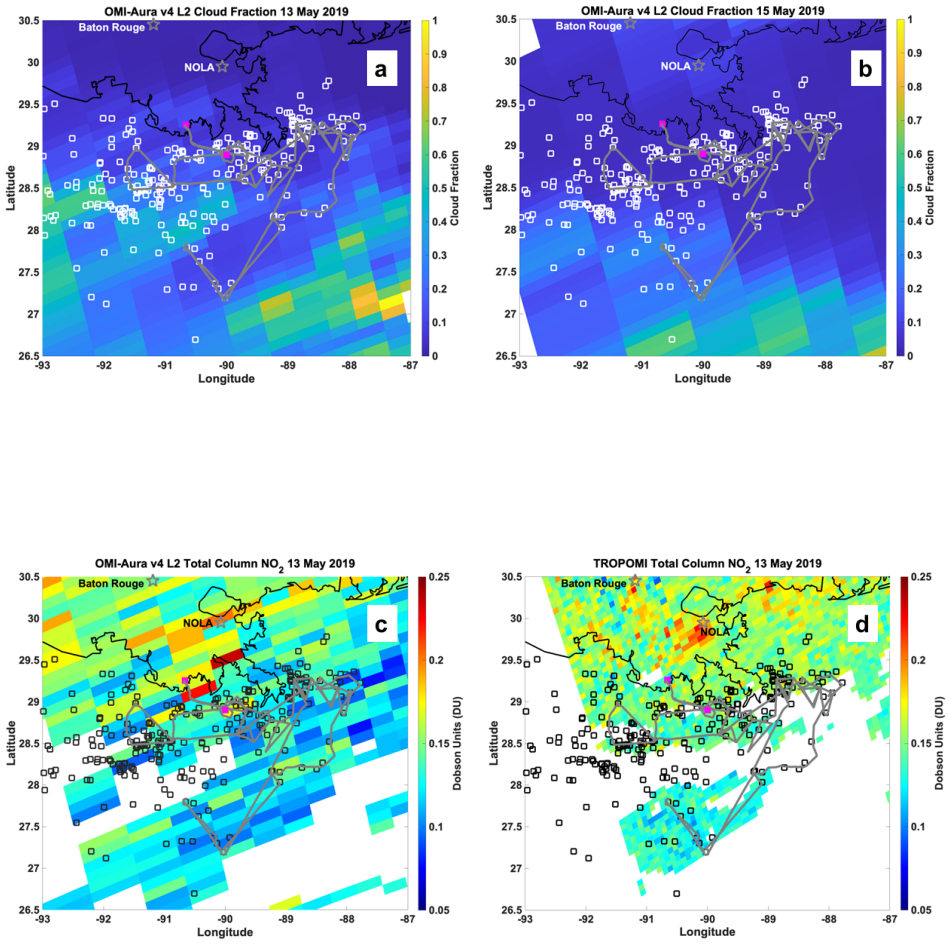

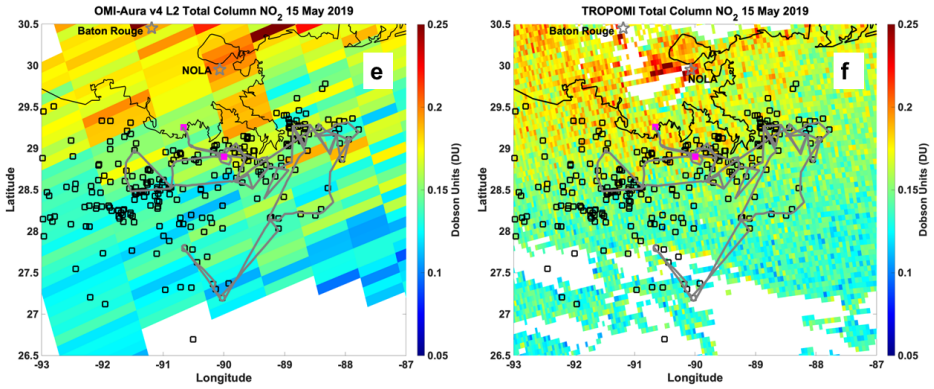

Figure 3. OMI v4 effective cloud fraction over SCOAPE cruise region on (a) 13 May 2019 and (b) 15 May 2019. Total Column (TC) NO_2 (DU) over SCOAPE cruise region on 13 May 2019 for (c) OMI v4 and (d) TROPOMI v1.3 observations. Total Column (TC) NO_2 (DU) on 15 May 2019 for (e) OMI v4 and (f) TROPOMI v1.3. In (c) through (f) black open squares are the locations of the top 500 NO_x-emitting platforms from BOEM's 2014 inventory (*Wilson et al.,* 2017); white open squares mark the same in (a) and (b). The gray solid line marks the *R/V Point Sur* cruise track. The cities of New Orleans, Louisiana (NOLA), and Baton Rouge, Louisiana, are indicated with open gray stars.

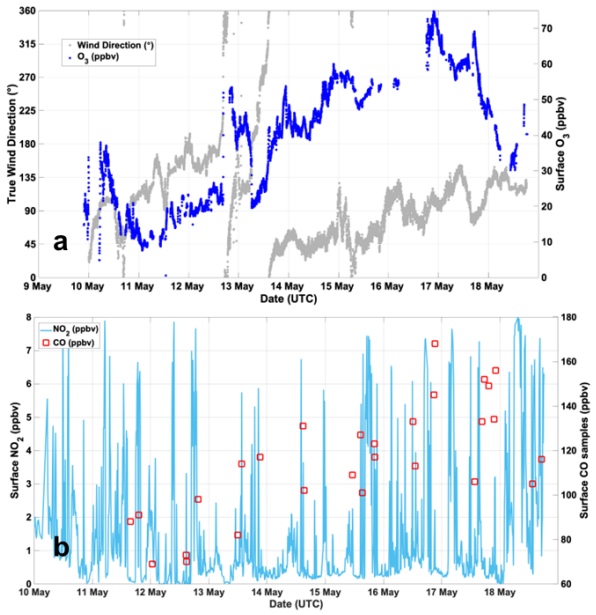

Figure 4. (a) Ozone mixing ratio (right scale) in ppbv with wind direction (left scale, in degrees) measured on *R/V Point Sur* during May 2019 cruise (presented as 5-minute means); (b) NO_2 mixing ratio (left scale; 15-minute means) in ppbv with CO mixing ratio in ppbv from canister samples taken along the *R/V Point Sur* track.

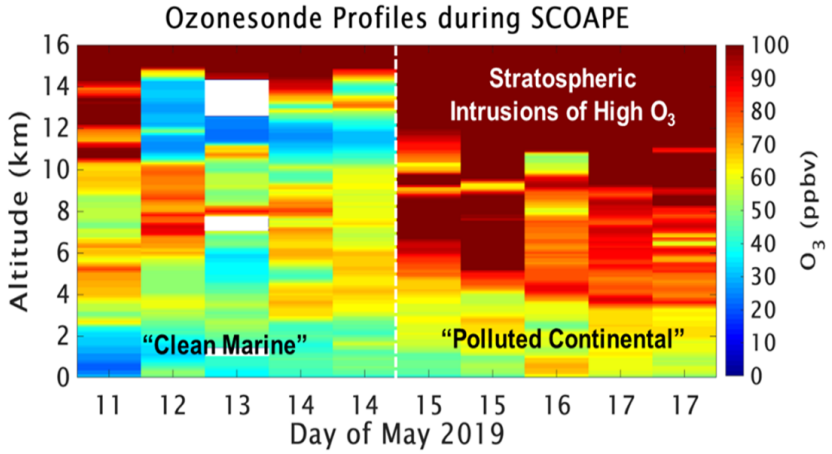

Figure 5. Ozonesonde profiles, during SCOAPE, based on 0.25 km resolution data. Mixing ratios to 16 km are illustrated; layers with > 80 ppbv may signify

stratospheric influence. Blue colors are concentrations associated with tropical marine boundary layer. On 12-14 May ozone concentrations 20-30 ppbv above 10 km are typical of air parcels in which deep convection introduced boundary layer air.

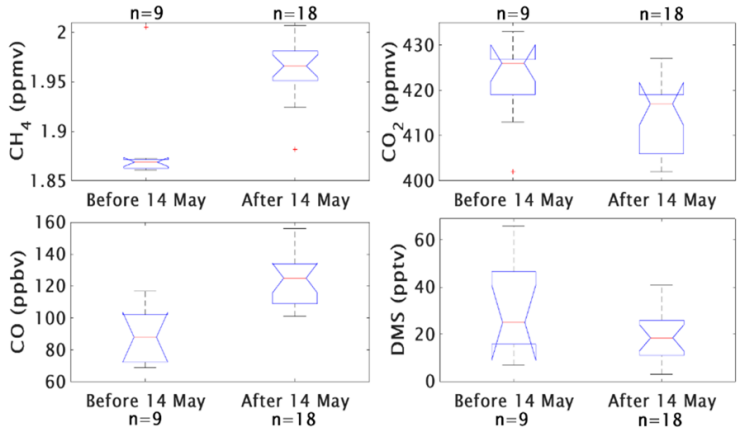

Figure 6. Box and whisker panels for CH_4, CO, CO_2 and dimethylsulfide (DMS) before (left side of each panel) and after 14 May (right side of each panel). Sample numbers indicated at the top or bottom of each panel. Red line denotes median values, blue box denotes 25^{th} and 75^{th} percentile, and whiskers (dashed bars) are 95^{th} percentile.

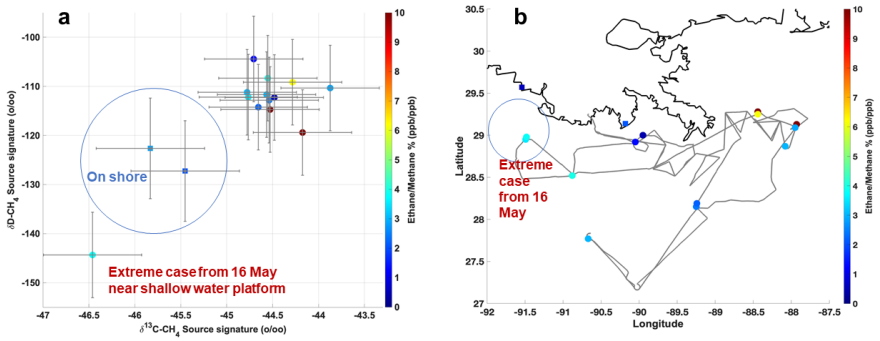

Figure 7. VOC canister observations of CH_4 isotope source signatures for ship (circles) and coastal (squares) measurements 11-19 May 2019. Colormap indicates ethane to methane ratios (% (ppb/ppb)) in the scatter plot (a) and in the map (b). Error bars show 1-sigma.

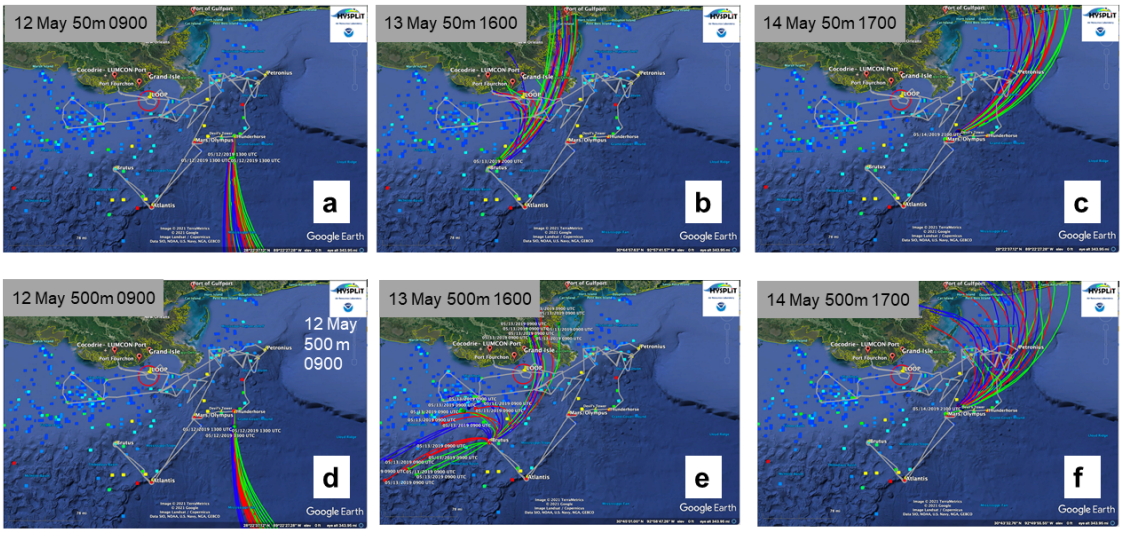

Figure 8. HYSPLIT 12-hour ensemble back trajectories released at 50m (top panels; a-c) and 500m (lower panels; d-f) at the local times listed in each (12-14 May 2019) and driven by the NCEP Global Data Assimilation System (GDAS) at 0.5-degree resolution. Colors of the trajectories denote change in ensemble trajectories' release time (every 3 hours over 12-hour period).

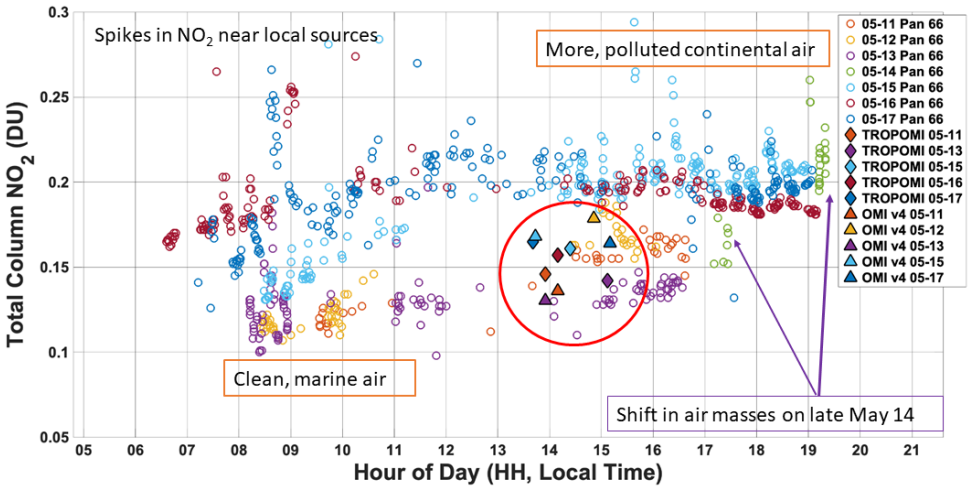

Figure 9. Pandora diurnal cycle of TC NO_2 during the cruise period 11-17 May 2019 (color of lines denotes day of observation) with TROPOMI overpass values (diamonds in corresponding day of cruise color) and OMI v4 overpass values (triangles in corresponding day of cruise color).

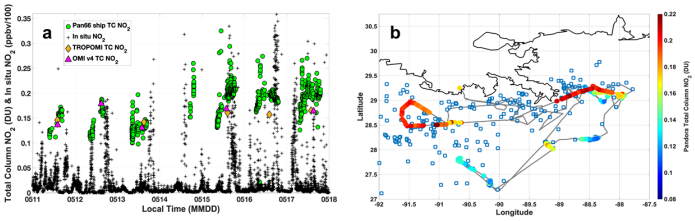

Fig 10. (a) Time series of TROPOMI, OMI v4, Pandora TC NO_2 and in situ NO_2 during SCOAPE cruise. Pandora TC NO_2 measurements and in situ data are 5-min averages. (b) Pandora TC NO_2 along ship track (in gray), 10-18 May 2019, during SCOAPE cruise. Blue squares mark the locations of platforms that fall into the category of the top 200 NO_x emitters according to the 2014 BOEM inventory (*Wilson et al.,* 2017). The cleaner air portion of the cruise, as shown

in Figures 4 and 5, was sampled prior to 14 May, more polluted air masses after 14 May.

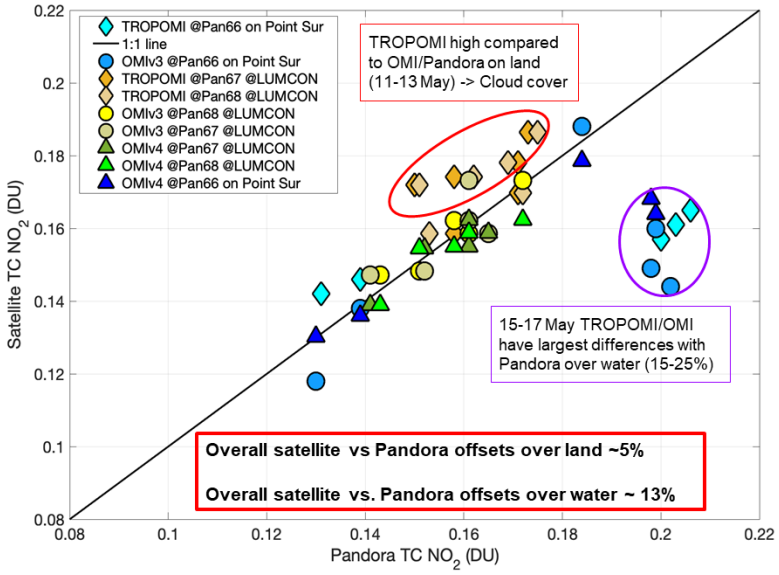

Figure 11. Satellites vs. Pandora 66 TC NO_2 on the *R/V Point Sur* during the cruise period 11-17 May 2019 with OMI v3 (light blue circles), OMI v4 (blue triangles), and TROPOMI v1.3 (cyan diamonds) readings referred to y-axis versus Pandora 66 on x-axis. Satellites vs. Pandora TC NO_2 at LUMCON 11-17 May 2019 with: OMI v3 versus Pandora 67 (light yellow circles) and 68 (yellow circles) on the x-axis; OMI v4 versus Pandora 67 (dark green triangles) and 68 (green triangles) on the x-axis; and TROPOMI v1.3 versus Pandora 67 (gold diamonds) and 68 (tan diamonds) on the x-axis.

Table 1. List of relevant campaigns and experiments that preceded SCOAPE.

Campaign (Year(s))	Geographic Location	Reference
CAPABLE (2009, 2010, 2011)	Hampton, VA	*Martins et al.* (2012) *Knepp et al.* (2015)
DISCOVER-AQ MD (2011)	Baltimore, MD -Washington, D.C.	*Reed et al.* (2015) *Tzortziou et al.* (2015)
DISCOVER-AQ TX (2013)	Houston, TX	*Flynn et al.* (2014) *Nowlan et al.* (2016) *Judd et al.* (2019)
DANCE (2014)	Atlantic Coast (DE-NC)	*Martins et al.* (2016) *Kollonige et al.* (2018)

Campaign (Year(s))	Geographic Location	Reference
KORUS-OC (2016)	Southern Korean peninsula	*Tzortziou et al.,* (2018) *Thompson et al.* (2019a)
LMOS (2017)	Lake Michigan	*Adelman et al.* (2020) *Stanier et al.* (2021)
OWLETS (2017)	Hampton, VA; Lower Chesapeake Bay	*Sullivan et al.* (2018) *Gronoff et al.* (2019) *Dacic et al.* (2020)
OWLETS-2 (2018)	Baltimore, MD; Upper Chesapeake Bay	*Sullivan et al.* (2020) *Kotsakis et al.* (2022)
LISTOS (2018)	Long Island Sound, NY	*Judd et al.* (2020) *Karambelas et al.* (2020)

Table 2. Offshore instrumentation on R/V Point Sur during SCOAPE cruise.

Species	Instrument	Collaborator
NO_2 (and calibrator)	In situ	NASA GSFC
Column NO_2	Pandora (PSI)	NASA GSFC (Swap*)
O_3	In situ Ozonesondes	NASA GSFC
Temperature, RH, etc.	Met system	R/V Point Sur
Aerosol (AOD) & O_3 columns	Microtops Columns	NASA GSFC
VOCs (plus CO & CH_4)	In situ canisters	UCI (Blake)
HCHO	In situ (Aeris)	NASA GSFC (Hanisco)
PBL height	Ceilometer	UMBC (Delgado)
Black carbon	Aethalometer	NIST (Conny)
CH_4, CO_2, H_2O	In situ (Picarro)	GSFC (Kawa / Hanisco)

* Collaborators for loaned instruments in parentheses.

Table 3. Onshore instrumentation during SCOAPE cruise.

Species	Instrument	Collaborator
NO_2	In situ analyzer	NASA GSFC (Sullivan)
NO_2	Mobile in situ (NO_2 sonde)	KNMI (Stein-Zweers/den Hoed)
Column NO_2	Pandora	NASA GSFC (Swap)
VOCs (plus CO & CH_4)	In situ canisters	UCI (Blake)
PBL height	Ceilometer	U Houston (Flynn)

Table 4. AQ conditions from VOC can sample on 16 May near shallow-water

platform at

(28.9795°, -91.4760°).

VOC Species	Cruise Median	16 May Plume Can	Notes
CH_4 (ppmv)	1.96	5.71	Deepwater platforms flare this off
CO_2 (ppmv)	415	418	No combustion, likely just leaky pipes
Ethane (ppbv)	2.1	145	C_2H_6; second largest component of fossil gas aft
Propane (ppbv)	0.7	90.1	C_3H_8; byproduct of fossil gas processing
n-Butane (ppbv)	0.3	29.9	C_4H_{10}; i-Butane had similar concentrations
Benzene (ppbv)	0.04	1.88	C_6H_6; known carcinogen